SIMULATING MICROSTRUCTURE-RELATED LCF VARIABILITY IN NICKEL-BASE SUPERALLOYS

R. S. KUMAR & D. L. McDOWELL
School of Mechanical Engineering, Georgia Institute of Technology, Atlanta, GA 30332-0405, USA

ABSTRACT

Dissipative microstructure rearrangement processes such as cyclic plasticity and formation of fatigue cracks are nonuniformly distributed within a heterogeneous material. Localization of deformation due to the heterogeneous nature of microstructure and multiple scales of precipitates are key factors influencing the low cycle fatigue (LCF) behavior of Ni-base superalloys at low to moderate temperatures. In this paper we focus on the cyclic deformation of Ni-base superalloy single crystal using a physically-based constitutive model, specifically examining the role of key microstructure attributes on the cyclic plastic shear strain localization. The local cyclic plastic shear strain distribution for different microstructures are compared and correlated with microstructural descriptors that permit assessment of relative fatigue resistance. Implications are drawn for microstructure-dependence of variability of fatigue resistance.

1 INTRODUCTION

It is well known that excellent mechanical properties of Ni-base superalloys at high temperatures are due to the hardening provided by coherent Ni_3Al precipitates in the microstructure. The precipitates are cuboidal in shape and their size distribution is usually bi-modal. Larger precipitates are referred to as primary (γ') and the smaller ones as secondary (γ''). In addition, there could be hyperfine precipitates called tertiary (γ'''). The size distribution, the spatial distribution and the volume fraction of the precipitates can be controlled using various heat treatments. The mechanical properties of Ni-base superalloys including LCF behavior and fatigue crack propagation rates are strongly affected by the volume fraction and microstructural attributes (size and spatial distribution) of the precipitates. These microstructural attributes can be controlled and tailored during the manufacturing processes to achieve an enhancement in the properties. Traditionally, one would adopt a trial-and-error approach based on intuition and large number of experiments - this is always expensive and time consuming. An alternative approach that is advocated in this work is to use computational simulations to guide the manufacturing strategies to achieve optimal microstructure with respect to given objectives. In this research, we use computational micromechanics to study the effects of variation in precipitate size and volume fraction on the LCF behavior at 650 °C. Such studies can provide guidelines to design the alloy for better LCF resistance.

2 CONSTITUTIVE MODEL

A physically-based crystal viscoplasticity constitutive model is used for both the precipitate and the matrix phases with dislocation density modeled as an internal variable. Anomalous yield stress behavior with respect to temperature and non-Schmid effects on flow stress in the precipitates are incorporated in the constitutive model. The non-local and directional nature of dislocation interactions with the precipitates during cyclic loading are modeled by explicit introduction of microstructure dependent length scales in the constitutive law for the matrix (or mixture of matrix and fine, nm scale precipitates). The constitutive model is implemented as a user material (UMAT) subroutine in ABAQUS [1] finite element package. The details of the models are presented in Wang et al. [2].

3 COMPUTATIONAL MODELING OF TWO-PHASE MICROSTRUCTURE

In this work we consider explicit modeling of cuboidal γ′ precipitates in a homogeneous matrix. The phases are modeled using the crystal plasticity-based constitutive model. The precipitates are considered to be randomly distributed in the matrix. This is in contrast to most of the existing work in the literature that assume periodic distribution and hence adopt a periodic unit cell model. It has been observed experimentally that the distribution of the precipitates, especially in polycrystalline Ni-base superalloys, is not periodic. As the computational cost of each finite element analysis is quite significant, we adopt 2-D domain for analysis. We consider a square domain for analysis and generate the distribution of square precipitates in it using a constrained Poisson's point process. The centroids of the precipitates are generated with the constraint that no two particles overlap. Furthermore, two precipitates are not allowed to be closer than a specified channel width or to intersect the boundary of the analysis domain. For a given size and volume fraction of the precipitates, three different realizations are generated so that scatter in the results due to finite window size can be studied.

The simulated microstructure is meshed in a finite element pre-processor for further analysis. In this work, we used ABAQUS/CAE (Abaqus, Inc., [1]) for meshing the simulated microstructures. The microstructures are imported automatically into ABAQUS/CAE using Python-based scripting language. The mesh is then generated manually within ABAQUS/CAE. In principle, the meshing process could be automated. However, in the present work this was not done as a user input was required to assure that the mesh is of acceptable quality. A free-mesh with linear triangular elements was used for all the simulations. The use of triangular element was necessary to mesh the complicated geometry of the microstructures. The mesh size was chosen based on a mesh convergence study. Generalized plane strain formulation was adopted for the finite elements with 3-D constitutive equations

The constitutive model for the matrix phase γ (with homogenized secondary and tertiary precipitates) has length-scale dependent terms in the dislocation density evolution relations [2]. In the explicit modeling of γ′ in homogenized γ, each slip system of an integration point within γ phase has a length-scale dependent term of the form

$$Z_o = \frac{k_{p\delta}}{b d_{p\delta}} \tag{1}$$

where b is the Burgers vector, $k_{p\delta}$ is a constant and $d_{p\delta}$ is the spacing associated with the γ′ precipitates. It is assumed that $k_{p\delta}$ and b are same for each of the octahedral and cubic slip systems as well as at each integration point of the matrix. However, the distance parameter $d_{p\delta}$ associated with the spacing of the γ′ precipitates is different on different slip systems. Furthermore the distance parameter is dependent on the location of the integration point within the mesh – an integration point in the narrow channel between two precipitates will have a smaller value of the distance parameter compared with an integration point located in the matrix rich region of the microstructure. The distance parameter on a particular slip system at an integration point is defined as the distance between the integration point and the nearest precipitate edge that is intersected by the slip system. In 2-D simulation, this is implemented by projecting the slip direction of the slip system on the simulation plane and checking its intersection with the γ′ precipitate. The intersection of the projected slip direction with nearest precipitates is identified. For each direction, we have two distance parameter: $d^{+}_{p\delta}$, associated with the intersection in the

direction of the slip and $d_{p\delta}^{-}$, associated with the intersection in the opposite (reverse) direction. If the slip direction of an integration point does not intersect any precipitate in the simulation window, its intersection with the adjacent windows is considered due to the doubly periodic nature of the boundary conditions. It is important to note that the positive and negative distance parameter associated with all slip systems of all the integration points in the γ matrix is assigned in the first increment of the first step in the analysis- this is essentially a pre-processing step. The information is stored in an array and later used within the UMAT to assign the correct distance depending on the current direction of the slip on the slip system. During cyclic loading, the slip direction changes sign and correct positive and negative distance is extracted from the stored values during the analysis procedure.

The finite element simulations are carried out on each realization of various simulated microstructures using ABAQUS/Implicit finite element code. The simulation temperature is taken to be 650 °C. The applied loading consists of fully reversed cyclic loading in the [001] direction. The loading is applied by means of prescribed displacement. The total strain range of 1.5% is applied and the loading strain rate is maintained at 0.5% s^{-1}. The simulations are carried out for 3 cycles as the stress-strain response is found to be stable after that.

In the computational modeling of heterogeneous domains, a number of different boundary conditions can be applied, namely, uniform traction, linear displacement, mixed and periodic. In the present case, we have adopted doubly periodic boundary condition. This boundary condition imposes constraints on the sides such that the opposite edges deform in the same manner. As the precipitates are randomly distributed within the domain and the boundary conditions are doubly-periodic, this boundary condition is also referred to as random-doubly periodic. This is different from boundary condition that enforces the edges to remain straight during the deformation process. The random-doubly periodic boundary condition allows the boundary to deform in any way as dictated by the heterogeneity within the simulation window and hence is more general. Of course, this boundary implies that the window (with randomly distributed heterogeneity) is repeated periodically in the x- and y-directions.

4 RESULTS AND DISCUSSION

It is known that LCF behavior of alloys is dictated by the distribution of cyclic plasticity in the microstructure. It has been found that cyclic plastic shear strain range correlates well with the formation of fatigue damage in metals and alloys [3]. To calculate this quantity at any integration point of the finite element mesh, we first consider a set of planes (directions) 10 degrees apart at that point. The plastic shear strain γ_θ^P on plane-θ is calculated by projecting the plastic strain tensor on it, i.e.,

$$\frac{\gamma_\theta^P}{2} = n_i \varepsilon_{ij}^P t_j \qquad \theta = 1 \ldots N , \tag{2}$$

where ε_{ij}^P is the plastic strain tensor at the integration point, n_i is the unit normal vector on plane-θ, t_i is a unit tangent vector in the considered direction along this plane, and N is the number of discrete planes. The cyclic range of the plastic shear strain on any plane is calculated in the third (stabilized) cycle of the simulation. First the range of the ratcheting component of plastic shear strain on the θ-plane is computed as

$$\Delta\gamma_\theta^{PR} = \left| \gamma_\theta^P \Big|_{\text{End of 3 Cycle}} - \gamma_\theta^P \Big|_{\text{Start of 3 Cycle}} \right|. \tag{3}$$

The maximum range of plastic shear strain on this plane is given by

$$\Delta\gamma_\theta^{PM} = \left| \max(\gamma_\theta^P) - \min(\gamma_\theta^P) \right|. \tag{4}$$

Now the cyclic plastic shear strain range on θ-plane associated with this integration point is obtained by subtracting the ratcheting component from the maximum range

$$\Delta\gamma_\theta^{PC} = \left| \Delta\gamma_\theta^{PM} - \Delta\gamma_\theta^{PR} \right|. \tag{5}$$

The contours of cyclic plastic shear strain range associated with all the planes can be plotted for each microstructure analyzed.

To compare different microstructure in terms of LCF resistance, we need to extract a measure of cyclic plastic shear strain range amongst all the different planes and amongst all the different regions (integration points) of the simulation window. One possibility is to take the maximum value amongst all the integration points and amongst all the planes. This measure is defined as

$$\Delta\gamma_{\theta,\max}^{PC} = \max_{IP,\theta} \left(\Delta\gamma_\theta^{PC} \right) \tag{6}$$

where 'IP' stands for all the integration points in the domain.

Even though the maximum value of cyclic plastic shear strain range can be used to compare different microstructures, it is not the most appropriate measure to correlate fatigue crack initiation lives as it is associated with a mathematical point hence it could be mesh-dependent. Furthermore fatigue crack incubation is associated with formation of persistent slip bands (PSBs) in the microstructure (cf. Venkataraman et al. [4]). The lower bound of minimum slip length over which fatigue crack may nucleate due to classical PSB formation may range from about 300 nm to 1000 nm. This establishes a minimum length scale over which some sort of averaging of cyclic plastic shear strain range must be carried out to obtain an appropriate physical measure to correlate incubation life. As the window size of simulation (statistical volume element, SVE) is of the order of the length scale for classical PSB formation, we propose a value of cyclic plastic shear strain range based on percolation of micro-plasticity within the SVE as an appropriate measure.

The percolation value of cyclic plastic shear strain range is calculated by first identifying the critical plane based on the peak value of cyclic plastic shear strain range amongst all the planes and all the integration points in the microstructure. Once the plane is identified, we determine the maximum value of cyclic plastic shear strain range such that the regions of the microstructure with cyclic plastic shear strain range greater than or equal to this specified value form a contiguous region spanning the opposite edges of the window. This maximum value of cyclic plastic shear strain range, $\Delta\gamma^{PC*}$, is defined as the quantity related to percolation of micro-plasticity.

4.1 Comparison of Different Microstructures

Two different microstructural attributes are analyzed – precipitate size and precipitate volume fraction. For a fixed volume fraction of 0.4, we consider four precipitate sizes 0.075, 0.1, 0.3 and 0.5 μm. For studying the effect of volume fraction effect, we fix the precipitate size to be 0.1 and 0.3 μm and for each of these, we consider three volume fractions 0.2, 0.3 and 0.4. Based on mesh convergence study, the average element size to precipitate size ratio was fixed at 0.133. Furthermore, we studied the window size effect on the two plastic shear strain range measure for one microstructure. Based on this study, the window size to precipitate size ratio was fixed at

10.67. The results of the simulations are presented in Figs. 1-3. In Fig. 1, the effect of precipitate size on cyclic plastic shear strain range is presented. Both the maximum and value at percolation are presented. The results illustrate that cyclic plastic shear strain range increases with the increase in the precipitate size. This increase is rapid at first but tend to saturate beyond the precipitate size of 0.3μm. This would imply that larger precipitate would have smaller LCF life. The effects of volume fraction are studied for two fixed precipitate sizes, namely 0.1μm and 0.3μm. Figure 2 presents the cyclic plastic shear strain range for 0.1μm precipitates and Fig. 3 presents the results for 0.3μm precipitates. It is observed from these results that increase in the precipitate volume fraction for a fixed precipitate size reduces the cyclic plastic shear strain range thereby increasing the LCF life. It is also noted that the decrease in cyclic plastic shear strain range with volume fraction is larger for smaller precipitate size.

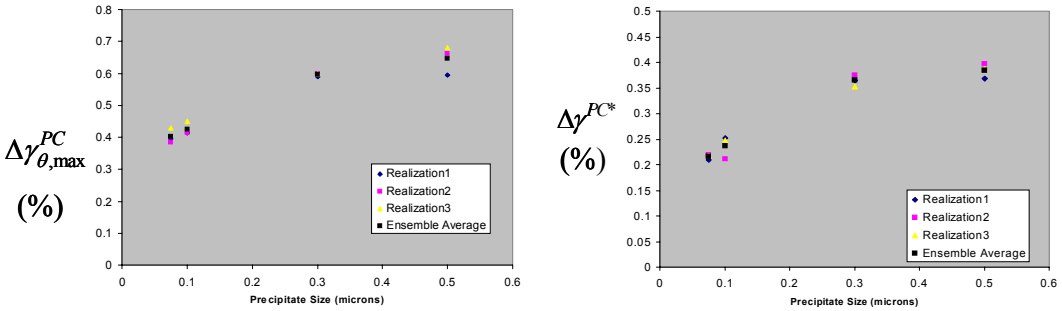

Fig. 1: Effect of precipitate size on cyclic plastic shear strain range at fixed volume fraction of 0.4.

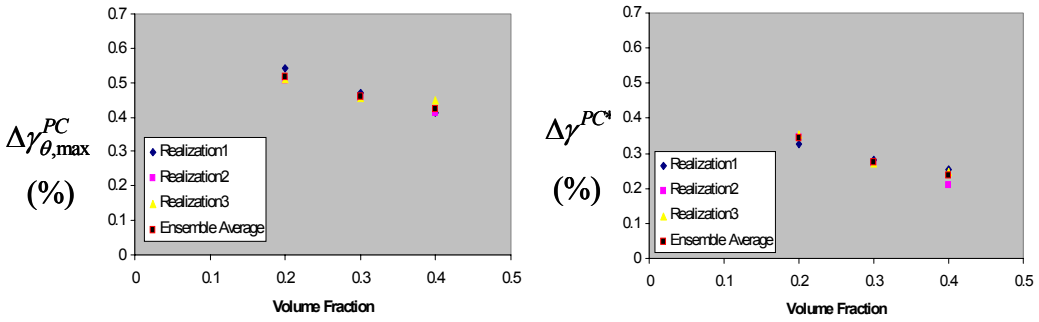

Fig. 2: Effects of precipitate volume fraction (precipitate size = 0.1μm).

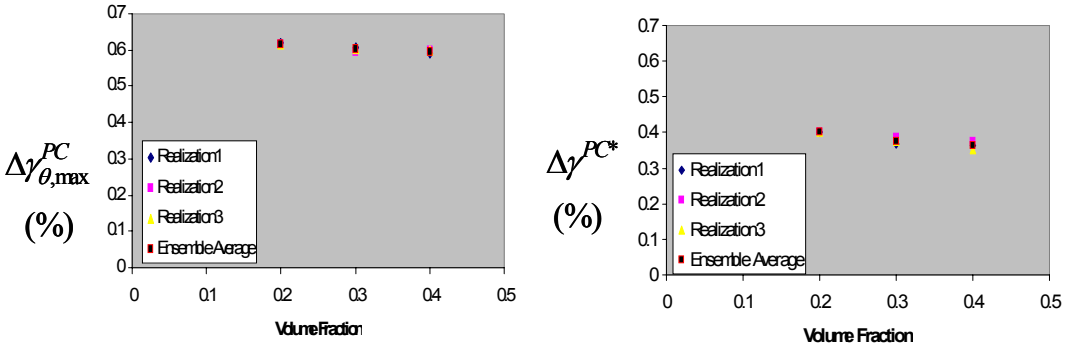

Fig. 3: Effects of precipitate volume fraction (precipitate size = 0.3μm).

5 CONCLUDING REMARKS

Understanding the role of microstructure on cyclic plasticity is important to design the microstructure for LCF resistance. In this paper, we used physically-based crystal viscoplastic constitutive models to study the effect of precipitate size, volume fraction and spatial distribution on cyclic plastic shear strain range under fully reversed cyclic loading at 650 °C. Two measures of cyclic plastic shear strain range – maximum and value at percolation – are used to compare various microstructures. The results show that cyclic plastic shear strain range increases with the increase in the precipitate size (for a fixed precipitate volume fraction) implying larger precipitates would result in smaller LCF life. On the other hand, increasing the volume fraction (at fixed precipitate size) results in smaller values of plastic shear strain range implying greater LCF life for higher precipitate volume fraction. The actual value of LCF lives can be calculated using a local Coffin-Manson relation connecting the measure of cyclic plastic shear strain range to the cycles to formation of a fatigue crack.

6 REFERENCES

[1] ABAQUS, Version 6.3-1., ABAQUS, Inc., Pawtucket, RI, 2002.

[2] Wang, A. -J., Kumar, R. S., Shenoy, M. M., McDowell, D. L., Microstructure-Based Constitutive Modeling of Two-Phase Nickel-Base Superalloys, Manuscript under preparation.

[3] Gall, K., Horstemeyer, M. F, Degner, B. W., McDowell, D. L., and Fan, J., On the Driving Force for Fatigue Crack Formation from Inclusions and Voids in a Cast A356 Aluminum Alloy, International Journal of Fracture, v108, pp. 207-233, 2001.

[4] Venkataraman, G., Chung, Y. W., Mura, T., Application Of Minimum Energy Formalism In A Multiple Slip Band Model For Fatigue - I. Calculation of Slip Band Spacings, Acta Metallurgica Materialia, v39(11), pp. 2621-2629, 1991; II. Crack Nucleation and Derivation of a Generalised Coffin-Manson Law, Acta Metallurgica Materialia, v39(11), pp. 2631-2638, 1991.